ISSN (e): 2250 – 3005 || Volume, 07 || Issue, 06|| June – 2017 ||
International Journal of Computational Engineering Research (IJCER)

Nature of Casson Fluid on Transient Free Convection Flow Past Towards an Impulsively Started Vertically Inclined Plate: Thermal Diffusion and Magnetic Field Effects

P.Suresh*, M. V. Ramana Murthy, S.Harisingh Naik, K Sreeram Reddy
Department of Mathematics& Computer Science, University College for Sciences, Osmania University, Hyderabad, 500007, Telangana State, India.
**Department of Mathematics, Chaitanya Bharathi Institute of Technology, Gandipet, Hyderabad, Rangareddy*

ABSTRACT

The aim of present investigation is to study the nature of Casson fluid on MHD free convective flow of over an impulsively started infinite vertically inclined plate with Soret, thermal radiation, heat and mass transfer effects. Assuming the medium to be non-scattered and the fluid to be non-gray, emitting-absorbing and optically thin radiation limit properties, the basic governing nonlinear coupled partial differential equations are solved numerically using finite difference method. The relevant physical parameters appearing in velocity, temperature and concentration profiles are analyzed and discussed through graphs. We also computed the Nusselt and Sherwood numbers along with friction factor for the same cases. Finally, the results for velocity profiles and the reduced Nusselt and Sherwood numbers are obtained and compared with previous results in the literature and are found to be in excellent agreement. Applications of the present study would be useful in magnetic material processing and chemical engineering systems.

Nomenclature:
List of variables:

B_0	Uniform magnetic field (*Tesla*)
x'	Coordinate axis along the plate (m)
y'	Co-ordinate axis normal to the plate (m)
u'	Velocity component in x' – direction ($m\ s^{-1}$)
T'	Fluid Temperature (K)
T'_w	Fluid temperature at the wall (K)
T'_∞	Fluid temperature away from the plate (K)
C'	Fluid Concentration ($Kg\ \ m^{-3}$)
C'_w	Concentration of the plate ($Kg\ \ m^{-3}$)
y	Dimensionless displacement (m)
C'_∞	Concentration of the fluid far away from the plate ($Kg\ \ m^{-3}$)
C_p	Specific heat at constant pressure $(J\ Kg^{-1}K)$
Cf	The local skin-friction ($N\ \ m^{-2}$)
Nu	The local Nusselt number
Sh	The local Sherwood number
u	Fluid velocity ($m\ \ s^{-1}$)
D_M	Solute mass diffusivity ($m^2\ \ s^{-1}$)
D_T	Mass diffusivity ($m^2\ \ s^{-1}$)
M	Magnetic field parameter
Gr	Grashof number for heat transfer
Gc	Grashof number for mass transfer
Pr	Prandtl number
Sc	Schmidt number
Sr	Soret number
Re	Reynolds number
g	Acceleration of gravity in magnitude, 9.81 ($m\ \ s^{-2}$)
t	Time (*sec*)
q_r	Radiative heat flux
$\vec{q}$	Velocity vector
P	Fluid pressure
$\vec{J}$	Electric current density vector
$\vec{B}$	Magnetic field vector
$\overline{E}$	Electric field vector
U_o	Reference velocity ($m\ \ s^{-1}$)
$\vec{g}$	Acceleration of gravity, 9.81 ($m\ \ s^{-2}$)
Q	Thermal radiation parameter

$K_{\lambda w}$ Absorption coefficient

$e_{b\lambda}$ Plank's function

Greek Symbols:

γ Casson fluid parameter

ν Kinematic viscosity ($m^2\ s^{-1}$)

ϕ Species concentration ($Kg\ \ m^{-3}$)

ρ The constant density ($Kg\ \ m^{-3}$)

β Volumetric coefficient of thermal expansion (K^{-1})

β^* Volumetric Coefficient of thermal expansion with concentration ($m^3\ Kg^{-1}$)

σ Electric conductivity of the fluid ($s\ m^{-1}$)

Θ Fluid temperature (K)

ϕ Fluid Concentration ($Kg\ \ m^{-3}$)

α Angle of inclination of plate (deg *rees*)

τ'_w Shear stress ($N\ \ m^{-2}$)

κ Thermal conductivity of the fluid $(W\ /\ mK\ )$

μ Coefficient of viscosity $(m.Pa.s)$

φ Dissipation of energy per unit volume due to viscosity

Superscripts:

$'$ Dimensionless Properties

Subscripts:

w Conditions on the wall

∞ Free stream conditions

p Plate

I. INTRODUCTION

The theory of non-Newtonian fluid is a part of fluid mechanics based on the continuum theory that a fluid particle may be considered as continuous in a structure. Pseudo plastic time independent fluid is one of the non-newtonian fluids whose behaviour is that viscosity decreases with increasing velocity gradient e.g. polymer solutions, blood, etc. Casson fluid is one of the pseudoplastic fluids that means shear thinning fluids. At low shear rates the shear thinning fluid is more viscous than the Newtonian fluid, and at high shear rates it is less viscous. So, MHD flow with Casson fluid is recently famous. Casson [1] presented Casson fluid model for the prediction of the flow conduct of pigment-oil suspensions. Mukhopadhyay [2] discussed heat transfer flow of Casson fluid over nonlinearly stretching sheet. The numerical solutions are carried out by shooting method. She concluded that skin friction and temperature gradient are increasing functions of Casson fluid parameter. The steady state electrically conducting flow of Casson fluid over a stretching sheet in a porous medium is reported by Shawky [3]. In the subsequent year, Nadeem et al. [4] explored three dimensional electrically conducting boundary layer flow of Casson fluid over stretching sheet saturated in a porous medium. Khalid et al. [5] investigated the effects of magnetic field on free convection flow of Casson fluid over oscillating plate embedded in porous medium. Poornima et al. [6] considered the velocity slip at wall for Casson fluid over a porous stretching surface. They found that slip parameter decreases fluid velocity and enhances shear stress at the wall. The mechanism of slip condition on stagnation point flow of Casson fluid has been reported by Hayat et al. [7]. Nadeem et al. [8] explored the combined effects of partial slip and magnetic field on stagnation point flow of Casson fluid over stretching surface. They concluded that slip parameter reduces the velocity of fluid in the boundary region. Mukhopadhyay et al. [9] analyzed the heat transfer on Casson fluid flow on a symmetric wedge. Oyelakin et al. [10] studied unsteady convective Casson nanofluid flow over a stretching sheet in the presence of thermal radiation and slip boundary conditions. Sailaja et al. [11] studied double diffusive effects on MHD mixed convection casson fluid flow towards a vertically inclined plate filled in porous medium in presence of Biot number using finite element technique. Srinivasa Raju et al. [12] discussed the influence of angle of inclination on unsteady MHD casson fluid flow past a vertical surface filled by porous medium in presence of constant heat flux, chemical reaction and viscous dissipation.

The assumption of Soret or thermal diffusion effect is valid when the concentration level is very low. The thermal diffusion effect (also known as Soret effect) is merely due to the effect of mass flux that occurs under a temperature gradient, and this phenomenon is utilized for isotope separation. The experimental investigation on this effect was first performed by Charles Soret in 1879. In mixtures between gases with very light molecular weight (H_2, *He*) and medium molecular weight (N_2, *Air*), the thermal diffusion is found to be of a magnitude such that it cannot be neglected as was emphasized by Eckert and Drake [13]. Srinivasa Raju [14] studied the effects of Soret and Dufour on natural convective fluid flow past a vertical plate embedded in porous medium in presence of thermal radiation via finite element method. Anand Rao et al. [15] studied finite element analysis of unsteady MHD free convection flow past an infinite vertical plate with Soret, Dufour, thermal radiation and heat source. Ahmed [16] found exact solutions of MHD transient free convection and mass transfer flow of a viscous, incompressible, and electrically conducting fluid past a suddenly started infinite vertical plate taking into account the thermal diffusion as well as the thermal radiation using Laplace transform technique. The influence of Soret and Dufour effects on flow field in free convection boundary layer from a vertical surface

embedded in a Darcian porous medium has been studied by Postelinicu [17]. Pal and Mondal [18] studied the MHD non-Darcy mixed convective diffusion of species over a stretching sheet embedded in a porous medium with non-uniform heat source/sink, variable viscosity and Soret effect. Thermophoresis particle deposition in a non-Darcy porous medium under the influence of Soret, Dufour effects studied by Partha [19]. Hayat et al. [20] examined the Soret and Dufour effects in three-dimensional flow over an exponentially stretching surface with porous medium, chemical reaction and heat source/sink. The steady and unsteady mixed convection with Sore and Dufour effects on chemically reacting MHD flow past a vertical plate embedded in porous medium studied by Makinde ([21]-[24]). Pal and Mondal [25] analyzed the chemical reaction and thermal radiation on mixed convection heat and mass transfer over a stretching sheet in Darcian porous medium with Soret and Dufour effects. Bourich et al. [26] studied analytically and numerically the Soret effect on the onset of convection in a vertical porous layer subjected to uniform heat flux.

The novelty of the present paper is to study the effects of Soret and thermal radiation on unsteady free convection non-Newtonian Casson fluid flow past an impulsively started infinite vertically inclined plate in the presence of magnetic field, heat and mass transfer effects. Non-dimensional quantities are introduced in the governing equations. The nonlinearity of the basic equations and additional mathematical difficulties associated with it, have led us to use numerical method. The transformed dimensionless governing equations are solved numerically by using finite difference method. The effects of various physical parameters on velocity, temperature, concentration profiles as well as on skin-friction, Nusselt number and Sherwood number are analyzed.

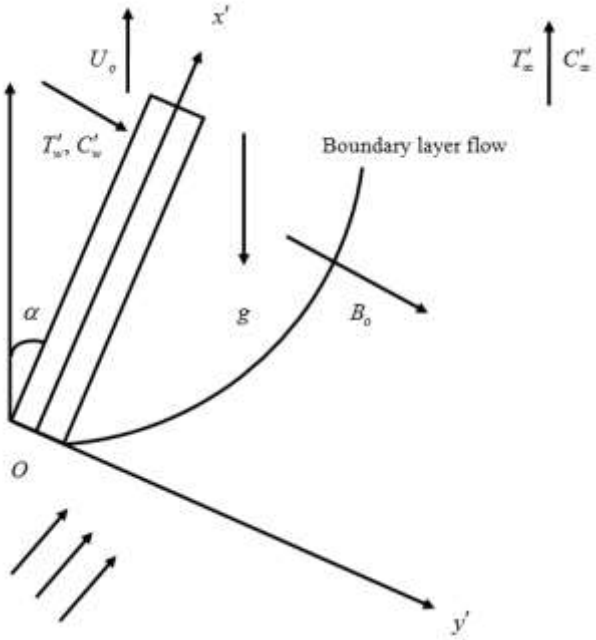

Fig. 1. Schematic view of flow configuration

II. MATHEMATICAL FORMULATION:

The fundamental governing equations in vector form of the motion of an incompressible, viscous, electrically conducting radiating Casson fluid flow past an impulsively started infinite vertically inclined plate in presence of a magnetic field are

Continuity Equation:

$$\nabla . \vec{q} = 0 \tag{1}$$

Momentum Equation:

$$\rho\left[\frac{\partial \vec{q}}{\partial t'} + (\vec{q}.\nabla)\vec{q}\right] = -\nabla P + \left(\vec{J} \times \vec{B}\right) + \rho\vec{g} + \mu\nabla^2\vec{q} \tag{2}$$

Energy Equation:

$$\rho C_p\left[\frac{\partial T'}{\partial t'} + (\vec{q}.\nabla)T'\right] = \kappa\nabla^2 T' + \varphi + \frac{\vec{J}^2}{\sigma} - \frac{\partial q_r}{\partial y'} \tag{3}$$

Species Concentration Equation:

$$\frac{\partial C'}{\partial t'} + (\vec{q}.\nabla)C' = D_M \nabla^2 C' + D_T \nabla^2 T' \quad (4)$$

Ohm's Law:

$$\vec{J} = \sigma\left(\vec{E} + \vec{q} \times \vec{B}\right) \quad (5)$$

We now consider an unsteady free convection Casson fluid flow of an incompressible, viscous, and electricity conducting past an impulsively started infinite vertically inclined plate in presence of a uniform transverse magnetic field of strength B_o, thermal radiation and Soret effects. Geometry of the problem is presented in Fig. 1. Our investigation is restricted to the following assumptions:

i. Coordinate system is chosen in such a way that $x'-$ axis is considered along the plate in upward direction and $y'-$ axis normal to the plate in the fluid.

ii. A uniform transverse magnetic field B_o is applied in a direction which is parallel to $y'-$ axis.

iii. Initially i.e., at time $t' \le 0$, both the fluid and plate are at rest and are maintained at a uniform temperature T'_∞.

iv. Also species concentration at the surface of the plate as well as at every point within the fluid is maintained at uniform concentration C'_∞.

v. The temperature at the surface of the plate is raised to uniform temperature T'_w and species concentration at the surface of the plate is raised to uniform species concentration C'_w and is maintained thereafter.

vi. All the fluid properties except the density in the buoyancy force term are constants.

vii. The viscous dissipation and Ohmic dissipation of energy are negligible.

viii. The magnetic Reynolds number is so small that the induced magnetic field can be neglected.

ix. Also no applied or polarized voltages exist so the effect of polarization of fluid is negligible.

The rheological equation of state for the Cauchy stress tensor of Casson fluid [27] is written as $\tau = \tau_0 + \mu\alpha^*$ (6)

equivalently
$$\tau_{ij} = \begin{cases} 2\left(\mu_B + \dfrac{p_y}{\sqrt{2\pi}}\right)e_{ij}, & \pi > \pi_c \\ 2\left(\mu_B + \dfrac{p_y}{\sqrt{2\pi_c}}\right)e_{ij}, & \pi < \pi_c \end{cases} \quad (7)$$

where τ is shear stress, τ_0 is Casson yield stress, μ is dynamic viscosity, α^* is shear rate, $\pi = e_{ij}e_{ij}$ and e_{ij} is the $(i,j)^{th}$ component of deformation rate, π is the product based on the non-Newtonian fluid, π_c is a critical value of this product, μ_B is plastic dynamic viscosity of the non-Newtonian fluid,

$$p_y = \frac{\mu_B\sqrt{2\pi}}{\gamma} \quad (8)$$

denote the yield stress of fluid. Some fluids require a gradually increasing shear stress to maintain a constant strain rate and are called Rheopectic, in the case of Casson fluid (Non-Newtonian) flow where $\pi > \pi_c$

$$\mu = \mu_B + \frac{p_y}{\sqrt{2\pi}} \quad (9)$$

Substituting Eq. (8) into Eq. (9), then, the kinematic viscosity can be written as

$$\nu = \frac{\mu}{\rho} = \frac{\mu_B}{\rho}\left(1 + \frac{1}{\gamma}\right) \quad (10)$$

Under the above foregoing assumptions and Boussinesq's approximation, the equations governing the flow and transport reduce to the following equations:

Continuity Equation:

$$\frac{\partial u'}{\partial x'} = 0 \Rightarrow u' = u'(y', t') \quad (11)$$

Momentum Equation:

$$\frac{\partial u'}{\partial t'} = \nu\left(1+\frac{1}{\gamma}\right)\frac{\partial^2 u'}{\partial y'^2} + g\beta(\cos\alpha)(T'-T'_\infty) + g\beta^*(\cos\alpha)(C'-C'_\infty) - \left(\frac{\sigma B_0^2}{\rho}\right)u'$$

(12)

Energy Equation:

$$\rho C_p \frac{\partial T'}{\partial t'} = \kappa \frac{\partial^2 T'}{\partial y'^2} - \frac{\partial q_r}{\partial y'} \qquad (13)$$

Species Diffusion Equation:

$$\frac{\partial C'}{\partial t'} = D_M \frac{\partial^2 C'}{\partial y'^2} + D_T \frac{\partial^2 T'}{\partial y'^2}$$

(14)

together with initial and boundary conditions

$$\left.\begin{array}{l} t' \le 0: u' = 0,\ T' = T'_\infty,\ C' = C'_\infty \quad for\ \ all\ \ y' \\ t' > 0: \left\{\begin{array}{l} u' = U_o,\ T' = T'_w,\ C' = C'_w \ \ at\ \ y' = 0 \\ u' = 0,\ T' = T'_\infty,\ C' = C'_\infty \ \ as\ \ y' \to \infty \end{array}\right. \end{array}\right\}$$

(15)

As mentioned earlier, in the case of optically thin limit, the fluid cannot absorb its own emitted radiation, but it absorbs the radiation emitted by boundaries. Following Cogley et al. [28], the rate of flux of radiation in the optically thin limit for a non-gray gas near equilibrium is given by

$$\frac{\partial q_r}{\partial y} = 4I(T'-T'_\infty) \qquad (16)$$

Where $I = \int_0^\infty K_{\lambda w}\left(\frac{de_{b\lambda}}{dT'}\right)d\lambda$.

We now introduce the following non-dimensional variables and parameters:

$$\left.\begin{array}{l} u = \frac{u'}{U_o},\ y = \frac{y'U_o}{\nu},\ t = \frac{t'U_o^2}{\nu},\ \theta = \frac{T'-T'_\infty}{T'_w-T'_\infty},\ \phi = \frac{C'-C'_\infty}{C'_w-C'_\infty},\ M = \frac{\sigma B_0^2\nu}{\rho U_o^2},\ Gr = \frac{g\beta\nu(T'_w-T'_\infty)}{U_o^3}, \\ Gc = \frac{\nu g\beta^*(C'_w-C'_\infty)}{U_o^3},\ \Pr = \frac{\nu\rho C_p}{\kappa},\ Sc = \frac{\nu}{D_M},\ Q = \frac{4I\nu^2}{\kappa U_o^2},\ Sr = \frac{D_T(T'_w-T'_\infty)}{\nu(C'_w-C'_\infty)},\ \mathrm{Re} = \frac{U_o x'}{\nu} \end{array}\right\}$$

(17)

The above defined non-dimensionless variables in Eq. (17) into Eqs. (12)-(14), and we get

$$\left(1+\frac{1}{\gamma}\right)\frac{\partial^2 u}{\partial y^2} - \frac{\partial u}{\partial t} - Mu + Gr(\cos\alpha)\theta + Gc(\cos\alpha)\phi = 0$$

(18)

$$\frac{\partial^2\theta}{\partial y^2} - (\Pr)\frac{\partial\theta}{\partial t} - Q\theta = 0 \qquad (19)$$

$$\frac{\partial^2\phi}{\partial y^2} - (Sc)\frac{\partial\phi}{\partial t} + (Sc)(Sr)\left(\frac{\partial^2\theta}{\partial y^2}\right) = 0 \qquad (20)$$

with connected initial and boundary conditions

$$\left.\begin{array}{l} t \le 0: u = 0,\ \theta = 0,\ \phi = 0 \quad for\ \ all\ \ y \\ t > 0: \left\{\begin{array}{l} u = 1,\ \theta = 1,\ \phi = 1 \ \ at\ \ y = 0 \\ u = 0,\ \theta = 0,\ \phi = 0 \ \ as\ \ y \to \infty \end{array}\right. \end{array}\right\} \qquad (21)$$

For the design of chemical engineering systems and practical engineering applications, the local skin-friction, Nusselt number and Sherwood number important physical parameters for this type of boundary layer flow. The Skin-friction at the plate, which in the non-dimensional form is given by

$$Cf = \left(1+\frac{1}{\gamma}\right)\frac{\tau'_w}{\rho v_o v} = \left(1+\frac{1}{\gamma}\right)\left(\frac{\partial u}{\partial y}\right)_{y=0} \quad (22)$$

The rate of heat transfer coefficient, which in the non-dimensional form in terms of the Nusselt number is given by

$$Nu = -x'\frac{\left(\frac{\partial T'}{\partial y'}\right)_{y'=0}}{T'_w - T'_\infty} \Rightarrow Nu\ \mathrm{Re}^{-1} = -\left(\frac{\partial \theta}{\partial y}\right)_{y=0} \quad (23)$$

The rate of mass transfer coefficient, which in the non-dimensional form in terms of the Sherwood number, is given by

$$Sh = -x'\frac{\left(\frac{\partial C'}{\partial y'}\right)_{y'=0}}{C'_w - C'_\infty} \Rightarrow Sh\ \mathrm{Re}^{-1} = -\left(\frac{\partial \phi}{\partial y}\right)_{y=0} \quad (24)$$

III. NUMERICAL SOLUTIONS BY FINITE DIFFERENCE METHOD:

The non-linear momentum and energy equations given in equations (18), (19) and (20) are solved under the appropriate initial and boundary conditions (21) by the implicit finite difference method. The transport equations (18), (19) and (20) at the grid point (i, j) are expressed in difference form using Taylor's expansion. The momentum equations reads.

$$\left(1+\frac{1}{\gamma}\right)\left(\frac{u_{i-1}^{j+1} - 2u_i^{j+1} + u_{i+1}^{j+1}}{2(\Delta y)^2} + \frac{u_{i-1}^{j} - 2u_i^{j} + u_{i+1}^{j}}{2(\Delta y)^2}\right) - \left(\frac{u_i^{j+1} - u_i^{j}}{\Delta t}\right)$$

$$+ (Gr)(\cos\alpha)\left(\frac{\theta_i^{j+1} + \theta_i^{j}}{2}\right) + (Gc)(\cos\alpha)\left(\frac{\phi_i^{j+1} + \phi_i^{j}}{2}\right) - M\left(\frac{u_i^{j+1} + u_i^{j}}{2}\right) = 0$$

(25)

$$\left(\frac{\theta_{i-1}^{j+1} - 2\theta_i^{j+1} + \theta_{i+1}^{j+1}}{2(\Delta y)^2} + \frac{\theta_{i-1}^{j} - 2\theta_i^{j} + \theta_{i+1}^{j}}{2(\Delta y)^2}\right) - (\mathrm{Pr})\left(\frac{\theta_i^{j+1} - \theta_i^{j}}{\Delta t}\right) - Q\left(\frac{\theta_i^{j+1} + \theta_i^{j}}{2}\right) = 0$$

(26)

$$\left(\frac{\phi_{i-1}^{j+1} - 2\phi_i^{j+1} + \phi_{i+1}^{j+1}}{2(\Delta y)^2} + \frac{\phi_{i-1}^{j} - 2\phi_i^{j} + \phi_{i+1}^{j}}{2(\Delta y)^2}\right) - (Sc)\left(\frac{\phi_i^{j+1} - \phi_i^{j}}{\Delta t}\right)$$

$$+ (Sr)(Sc)\left(\frac{\theta_{i-1}^{j+1} - 2\theta_i^{j+1} + \theta_{i+1}^{j+1}}{2(\Delta y)^2} + \frac{\theta_{i-1}^{j} - 2\theta_i^{j} + \theta_{i+1}^{j}}{2(\Delta y)^2}\right) = 0 \quad (27)$$

Where the indices i and j refer to y and t respectively. The initial and boundary conditions (21) yield:

$$\left.\begin{aligned} &u_i^0 = 0,\ \theta_i^0 = 0,\ \phi_i^0 = 0 \quad for\ all\ i, \\ &u_i^j = 1,\ \theta_i^j = 1,\ \phi_i^j = 1\ at\ i = 0\ \&\ u_M^j \to 0,\ \theta_M^j \to 0,\ \phi_M^j \to 0 \end{aligned}\right\}$$

(28)

Thus the values of u, θ and ϕ at grid point $t = 0$ are known; hence the temperature and concentration profiles have been solved at time $t_{i+1} = t_i + \Delta t$ using the known values of the previous time $t = t_i$ for all $i = 1, 2, ..., N-1$. Then the velocity field is evaluated using the already known values of temperature and concentration profiles obtained at $t_{i+1} = t_i + \Delta t$. These processes are repeated till the required solution of u, θ and ϕ is gained at convergence criteria.

$$abs\left|(u,\ \theta,\ \phi)_{exact} - (u,\ \theta,\ \phi)_{numerical}\right| < 10^{-3}$$

(29)

IV. VALIDATION OF CODE:

Table-1: Variation of the velocity profiles u against the Magnetic field parameter M.

M	Velocity profiles u					
	Present velocity results			Velocity results of Ahmed [16]		
	Gr = 0.0 and Gc = 0.0	Gr = 10.0 and Gc = 0.0	Gr = 0.0 and Gc = 5.0	Gr = 0.0 and Gc = 0.0	Gr = 10.0 and Gc = 0.0	Gr = 0.0 and Gc = 5.0
0.5	0.1149352461	0.6395227834	1.3592771636	0.114935	0.640697	1.36534
2.0	0.0924338153	0.4093348266	2.0138824461	0.091231	0.412131	2.012341
3.5	0.0219984315	0.2199834478	2.9786631995	0.022163	0.221357	2.98282
5.0	0.0124551830	0.1504433927	3.1620466317	0.01117	0.152467	3.176091
6.5	0.00593477150	0.1129375516	3.2588997114	0.006058	0.113079	3.268423

Table-2: Variation of the Nusselt number against Thermal radiation parameter Q.

Q	Present Nusselt number results		Nusselt number results of Ahmed [16]	
	Pr = 0.7	Pr = 7.0	Pr = 0.7	Pr = 7.0
0.5	0.7678511754	1.5881123347	0.77414	1.59808
1.0	1.0199831725	1.6998334775	1.02215	1.70101
1.5	1.2326881604	1.7966829513	1.23305	1.80162
2.0	1.4096678836	1.8820047848	1.41753	1.89999
2.5	1.5739943477	1.9804476277	1.58251	1.99621
3.0	1.7299604141	2.0845517325	1.73263	2.09038

Table-3: Variation of the Sherwood number against Soret number Sr at Pr = 0.7.

Sr	Present Sherwood number results		Sherwood number results of Ahmed [16]	
	Q = 0.0	Q = 3.0	Q = 0.0	Q = 3.0
0.0	0.4296551384	0.4296551384	0.437019	0.437019
0.5	0.3558175076	- 6.0428853742	0.363487	- 6.05382
1.0	0.2713380499	- 12.1058823445	0.289954	- 12.1076
1.5	0.2096177318	- 18.1564733805	0.216422	- 18.1615
2.0	0.1403177866	- 24.2094383176	0.142889	- 24.2153
2.5	0.0593376254	- 30.2598661347	0.0693566	- 30.2691
3.0	0.0041698275	- 36.3166804962	0.0041759	- 36.3229

V. RESULTS AND DISCUSSIONS:

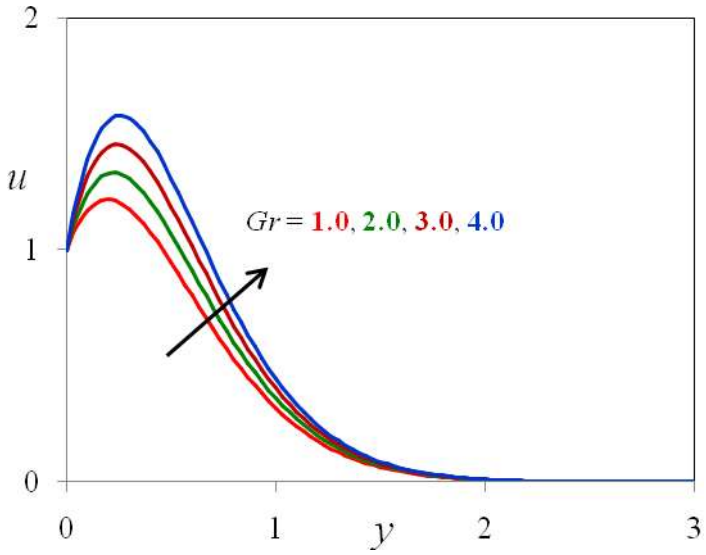

Fig. 2. Gr effect on velocity profiles

The formulation of the problem that accounts for the effects of thermal radiation and Soret on the Casson fluid flow past an impulsively started infinite vertically inclined plate in the presence of magnetic field was accomplished in the preceding sections. The governing equations of the flow field were solved numerically

using by finite difference method. In order to get physical insight into the problem, the velocity, temperature, and concentration fields have been discussed by assigning numerical values of Magnetic parameter M, Grashof number for heat transfer Gr, Grashof number for mass transfer Gc, Prandtl number Pr, Schmidt number Sc, Casson fluid parameter γ, Angle of inclination parameter α, Thermal radiation parameter Q and Soret number Sr. Throughout the calculations, the parametric values are fixed to be, $Gr = 2.0$, $Gc = 2.0$, $M = 0.5$, Pr = 0.71, $Sc = 0.22$, $Sr = 0.5$, $Q = 0.5$, $\gamma = 0.5$ and $\alpha = 45^{o}$ unless otherwise indicated.

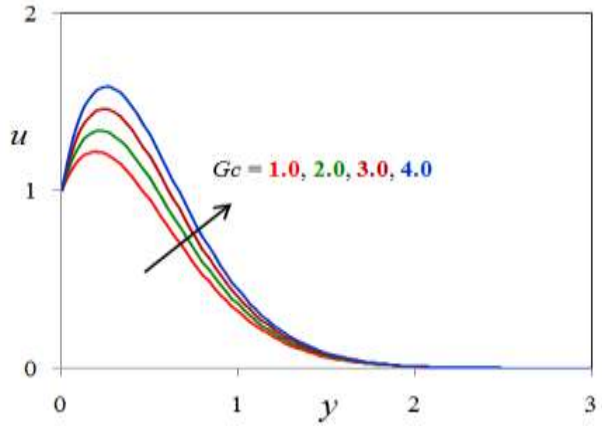

Fig. 3. *Gc* effect on velocity profiles

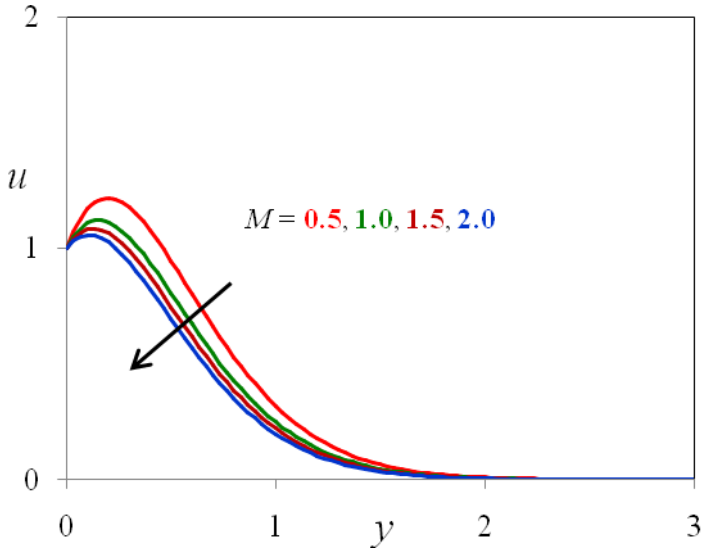

Fig. 4. *M* effect on velocity profiles

The velocity profiles for different values of Grashof number for heat transfer (Gr) is defined in Fig. 2. It is noticed that increase in Grashof number for heat transfer contributes to the increase in velocity of the fluid. Further, it is noticed in the boundary layer region the velocity first increases to a maximum value and then decreases. Also, far away from the plate, not much of significant effect of Grashof number for heat transfer is noticed. For the case of different values of the Grashof number for mass transfer (Gc), the velocity profiles in the boundary layer is shown in Fig. 3. The velocity distribution attains a distinctive maximum value in the vicinity of the plate and then decreases properly to approach a free stream value. As expected, the fluid velocity increases and the peak value becomes more distinctive due to increase in the buoyancy force represented by Gc, where as Gc increases, the velocity and the temperature increases. Fig. 4 illustrates the effect of magnetic field parameter M on velocity profiles in the boundary layer. It is interesting to note from Fig. 4 that the effect of Magnetic field is to decrease the value of the velocity profiles throughout the boundary layer. The peak value drastically decreases with increase in the value of the magnetic field, because, the presence of magnetic field in an electrically conducting fluid introduces a force called the Lorentz force, which acts against the flow if the magnetic field is applied in the normal direction. This type of resisting force slowdowns the fluid velocity as shown in the graph. The influence of Prandtl number Pr on the velocity profiles is illustrated in Fig. 5. It is observed that increase in Pr contributes to the decrease in the fluid velocity. The contribution by Pr is not that significant at the boundary. But the effect appears to be more significant as we move far away from the bounding surface.

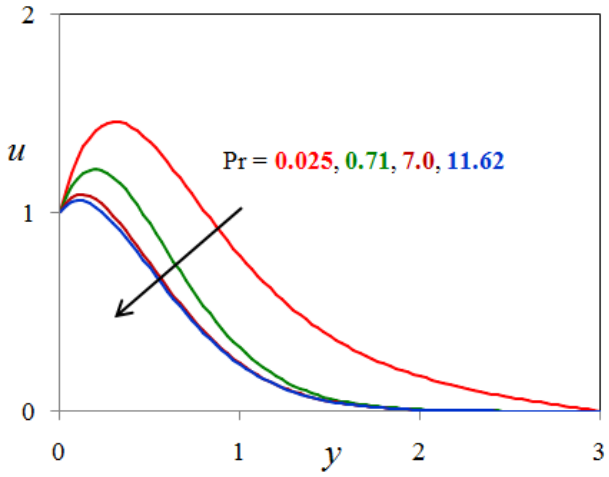

Fig. 5. Pr effect on velocity profiles

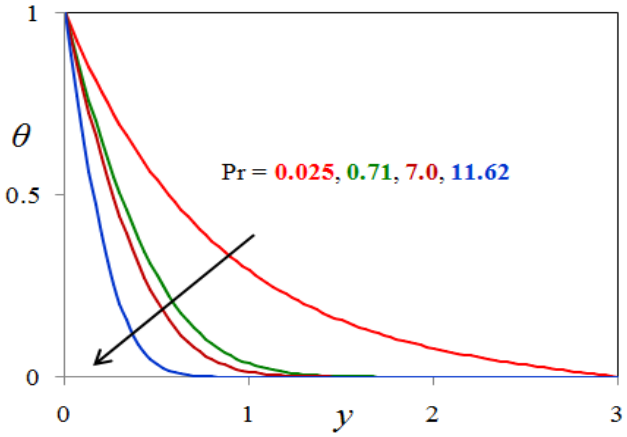

Fig. 6. Pr effect on temperature profiles

Fig. 6 illustrates the influence of Prandtl number on the temperature field. It is observed that the Prandtl number has significant contribution over the temperature field. From the illustrations it is seen that as the Prandtl number increases, the temperature decreases. From this plot it is evident that temperature in the boundary layer falls very quickly for large value of the Prandtl number, because of the fact that thickness of the boundary layer decreases with increase in the value of the Prandtl number. For different values of the Schmidt number *Sc*, the velocity profiles are plotted in Fig. 7. It is obvious that the effect of increasing values of *Sc* results in a decrease velocity profiles. Fig. 8 displays the effect of Schmidt number *Sc* on concentration profiles. Physically, the increase of *Sc* means decreases of molecular diffusion. Hence, the concentration of the species is higher for small values of *Sc* and lower for larger values of *Sc*.Therefore, as the Schmidt number increases the concentration decreases. This causes the concentration buoyancy effects to decrease, and there is a reduction in the fluid velocity.

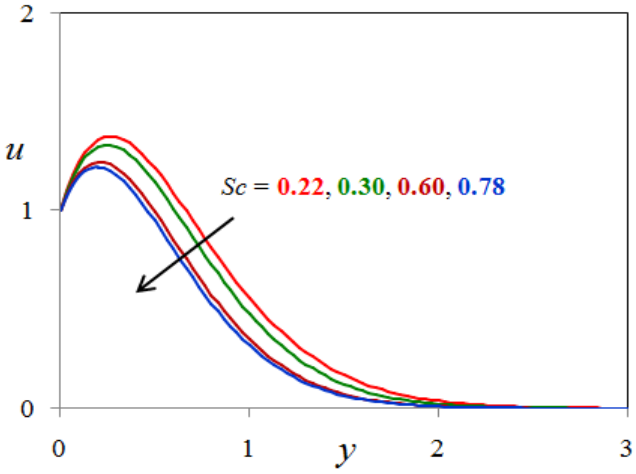

Fig. 7. *Sc* effect on velocity profiles

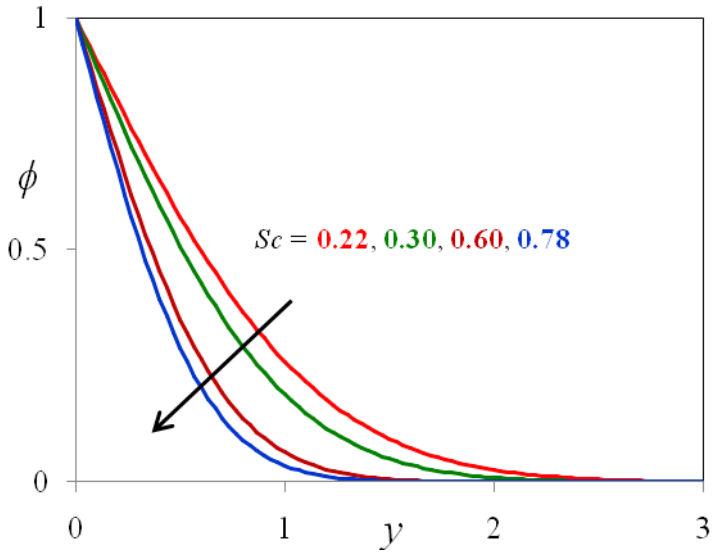

Fig. 8. *Sc* effect on concentration profiles

The contribution of Soret number *Sr* on the velocity profiles is noticed in Fig. 9. The increase in Soret number *Sr* contributes the increase in the velocity profiles. Further, it is noticed that the velocity decreases as we move away from the plate which is found to be independent of Soret number *Sr*. The influence of Soret number *Sr* on the concentration of the fluid medium is seen in Fig. 10. In general it is noted that increase in Soret number *Sr* contributes to increase in concentration of the fluid medium. Further, the effect is found to be diminishing as we move away from the plate. The effect of the thermal radiation parameter *Q* on the dimensionless velocity and temperature profiles are shown in Figs. 11 and 12 respectively.

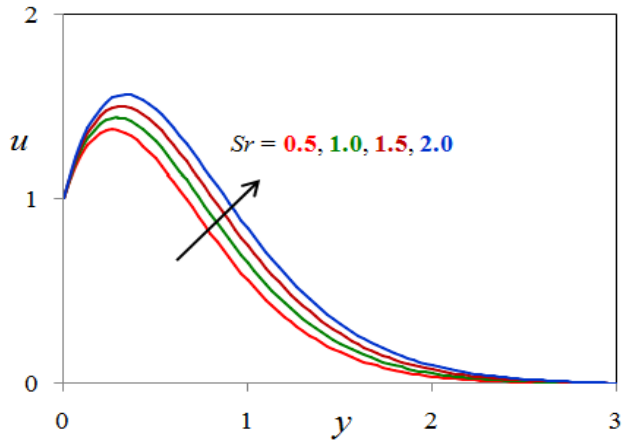

Fig. 9. *Sr* effect on velocity profiles

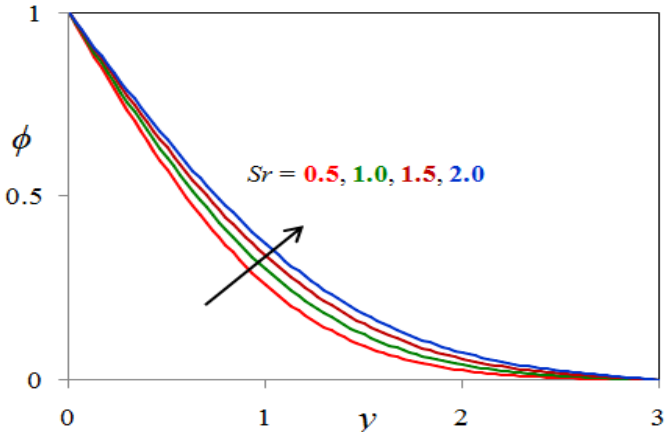

Fig. 10. *Sr* effect on concentration profiles

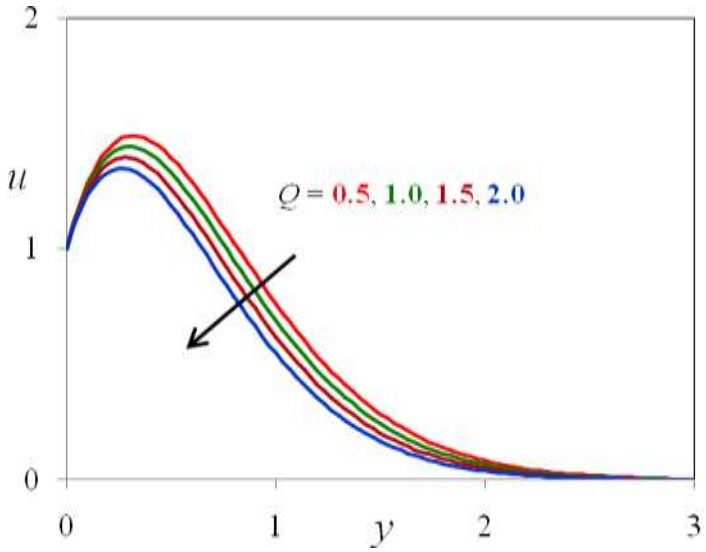

Fig. 11. *Q* effect on velocity profiles

Fig. 11 shows that velocity profiles decreases with an increase in the thermal radiation parameter Q. From Fig. 12, it is seen that the temperature decreases as the thermal radiation parameter Q increases. This result qualitatively agrees with expectations, since the effect of radiation is to decrease the rate of energy transport to the fluid, thereby decreasing the temperature of the fluid. The velocity profiles in the Fig. 13 shows that rate of motion is significantly reduced with increasing of Casson fluid parameter γ. Also, it is observed from this Fig. 13, the boundary layer momentum thickness decreases as increase of Casson fluid parameter γ. The effect of angle of inclination of the plate α on the velocity field has been illustrated in Fig. 14. It is seen that as the angle of inclination of the plate α increases the velocity field decreases.

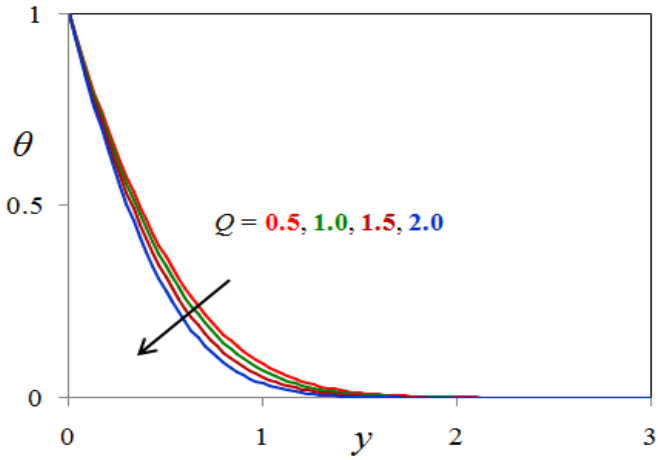

Fig. 12. *Q* effect on temperature profiles

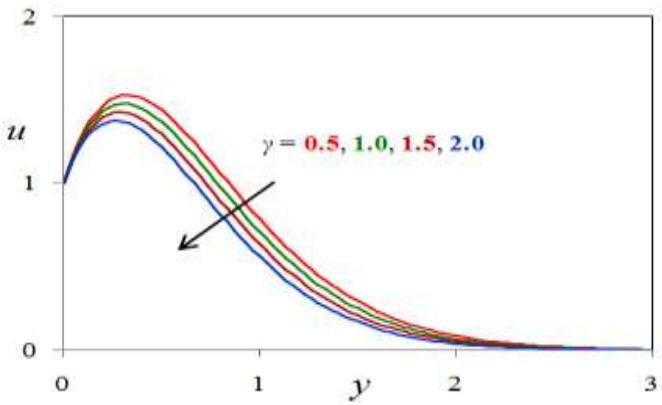

Fig. 13. γ effect on velocity profiles

The effects of Magnetic parameter *M*, Grashof number for heat transfer *Gr*, Grashof number for mass transfer *Gc*, Prandtl number Pr, Schmidt number *Sc*, Casson fluid parameter γ, Angle of inclination parameter α, Thermal radiation parameter *Q* and Soret number *Sr* on the skin-friction coefficient are portrayed in table 4. From this table, it is observed that the skin-friction coefficient increases as the Grashof number for heat transfer *Gr*, Grashof number for mass transfer *Gc* and Soret number *Sr* increases, whereas it decreases as the Magnetic parameter *M*, Prandtl number Pr, Schmidt number *Sc*, Casson fluid parameter γ, Angle of inclination parameter α and Thermal radiation parameter *Q*. The effects of the thermal radiation parameter *Q* and Prandtl number Pr on rate of heat transfer coefficient or Nusselt number are presented in table 5. From this table, it is noticed that the Nusselt number decreases as thermal radiation parameter *Q* and Prandtl number Pr increases. The effects of Soret number *Sr* and Schmidt number *Sc* on rate of mass transfer coefficient or Sherwood number are presented in table 5. From this table, it is observed that the Sherwood number increases as Soret number *Sr* increases, whereas it decreases as Schmidt number *Sc* increases.

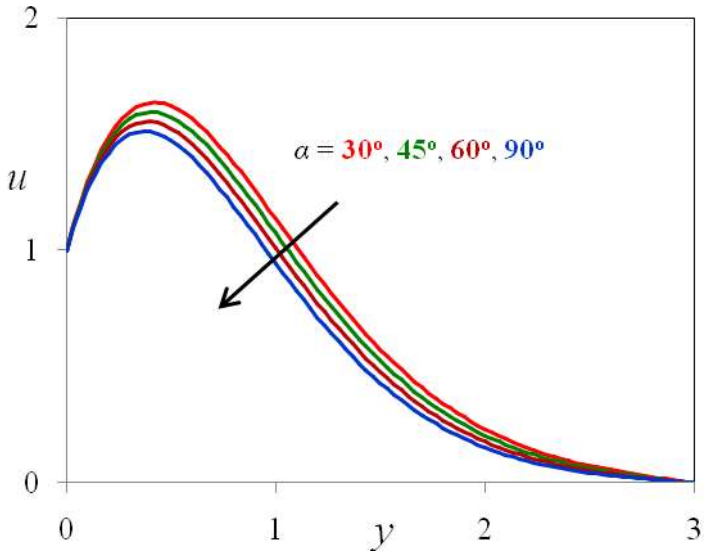

Fig. 14. α effect on velocity profiles

Table-4: Numerical values of Skin-friction coefficient

Gr	*Gc*	*M*	Pr	*Sc*	*Sr*	*Q*	γ	α	*Cf*
2.0	2.0	0.5	0.71	0.22	0.5	0.5	0.5	45^o	1.1035664851
4.0	2.0	0.5	0.71	0.22	0.5	0.5	0.5	45^o	1.2549554768
2.0	4.0	0.5	0.71	0.22	0.5	0.5	0.5	45^o	1.2764995132
2.0	2.0	1.0	0.71	0.22	0.5	0.5	0.5	45^o	1.0638816277
2.0	2.0	0.5	7.00	0.22	0.5	0.5	0.5	45^o	1.0863412773
2.0	2.0	0.5	0.71	0.30	0.5	0.5	0.5	45^o	1.0731996247
2.0	2.0	0.5	0.71	0.22	1.0	0.5	0.5	45^o	1.1206475103
2.0	2.0	0.5	0.71	0.22	0.5	1.0	0.5	45^o	1.0730551308
2.0	2.0	0.5	0.71	0.22	0.5	0.5	1.0	45^o	1.0920477136
2.0	2.0	0.5	0.71	0.22	0.5	0.5	0.5	60^o	1.0931750622

Table-5: Numerical values of rate of heat and mass transfer coefficients

Pr	*Q*	*Nu*	*Sc*	*Sr*	*Sh*
0.71	0.5	0.7739916785	0.22	0.5	0.3596244785
7.00	0.5	0.7329788304	0.30	0.5	0.3160472197
0.71	1.0	0.7531704485	0.22	1.0	0.3760083218

VI. CONCLUSIONS

The effects of thermal radiation and Soret on an unsteady free convection boundary layer flow of an electrically conducting Casson fluid past an impulsively started vertically inclined plate, by taking magnetic field, heat and mass transfer into account. The resultant governing partial differential equations are then solved numerically using finite difference method. The effects of governing thermo physical parameters on the velocity, temperature and concentration as well as Skin-friction, Nusselt number and Sherwood number are computed and

presented in graphical and tabular forms. The results and discussion of the present study leads to the following observations.

1. The velocity profiles are increasing with increasing values of Grashof number for heat transfer *Gr* and Grashof number for mass transfer *Gc*.
2. The effect of increasing the Prandtl number Pr, Schmidt number *Sc*, the Casson fluid parameter γ, the Angle of inclination parameter α, the Thermal Radiation parameter *Q*, the Magnetic field parameter *M* decelerates the velocity of the flow field at all points, while a growing the Soret number *Sr* accelerates the velocity of the flow field at all points.
3. A growing the Prandtl number Pr and Thermal radiation parameter *Q* are to retard the temperature of the flow field at all points.
4. The Concentration of the flow decreases with increasing values of the Schmidt number *Sc*, where as it increases with increasing values of Soret number *Sr*.
5. The skin-friction coefficient decreases when Prandtl number Pr, Schmidt number *Sc*, the Casson fluid parameter γ, the Angle of inclination parameter α, the Thermal Radiation parameter *Q*, the Magnetic field parameter *M* are increases, where as it increases with increasing values of Soret number *Sr*.
6. As the Prandtl number Pr and thermal radiation parameter *Q* increases, the rate of heat transfer coefficient or Nusselt number decreases.
7. Increase in the Schmidt number *Sc* results in a decrease in the rate of mass transfer coefficient or Sherwood number, where as it increases with increasing values of Soret number *Sr*.
8. The numerical results obtained and compared with formerly reported cases available in the open literature and they are found to be in very good concurrence.

REFERENCES

[1]. N. Casson, A flow equation for the pigment oil suspensions of the printing ink type, Rheology of Disperse Systems, Pergamon, New York (1959), pp. 84–102.

[2]. S. Mukhopadhyay, Casson fluid flow and heat transfer over a nonlinearly stretching surface, Chin. Phys. B, Vol. 22 (2013) http://doi.org/10.1088/1674-1056/22/7/074701.

[3]. H.M. Shawky, Magnetohydrodynamic Casson fluid flow with heat and mass transfer through a porous medium over a stretching sheet, J. Porous Media, 15 (2012), pp. 393–401.

[4]. S. Nadeem, R.U. Haq, N.S. Akbar, Z.H. Khan, MHD three-dimensional Casson fluid flow past a porous linearly stretching sheet, Alexandria Eng. J., 52 (2013), pp. 577–582.

[5]. A. Khalid, I. Khan, A. Khan, S. Shafie, Unsteady MHD free convection flow of Casson fluid past over an oscillating vertical plate embedded in a porous medium, Eng. Sci. Technol. Int. J., 80 (2015), pp. 1–9.

[6]. T. Poornima, P. Sreenivasulu, N.B. Reddy, Slip flow of casson rheological fluid under variable thermal conductivity with radiation effects, Heat Transf. Res., 44 (2014), pp. 718–737.

[7]. T. Hayat, M. Farooq, A. Alsaedi, Thermally stratified stagnation point flow of Casson fluid with slip conditions, Int. J. Numer. Methods Heat Fluid Flow, 25 (2015), pp. 724–748.

[8]. S. Nadeem, R. Mehmood, N.S. Akbar, Combined effects of magnetic field and partial slip on obliquely striking rheological fluid over a stretching surface, J. Magn. Magn. Mater., 378 (2015), pp. 457–462.

[9]. S. Mukhopadhyay, I. Mondal, A.J. Chamkha, Casson fluid flow and heat transfer past a symmetric wedge Heat Transf – Asian Res, 42 (2013), pp. 665–675.

[10]. Oyelakin, S. Mondal, P. Sibanda, Unsteady Casson nanofluid flow over a stretching sheet with thermal radiation, convective and slip boundary conditions, Alexandria Eng J, 55 (2) (2016), pp. 1025–1030.

[11]. S. V. Sailaja, B. Shanker, R. Srinivasa Raju, Double Diffusive Effects On MHD Mixed Convection Casson Fluid Flow Towards A Vertically Inclined Plate Filled In Porous Medium In Presence Of Biot Number: A Finite Element Technique, Journal of Nanofluids, Vol. 6, pp. 420 - 435, 2017.

[12]. R. Srinivasa Raju, B. Mahesh Reddy, G. Jithender Reddy, Influence Of Angle Of Inclination On Unsteady MHD Casson Fluid Flow Past A Vertical Surface Filled By Porous Medium In Presence Of Constant Heat Flux, Chemical Reaction And Viscous Dissipation, Journal of Nanofluids, Vol. 6, pp. 668 - 679, 2017.

[13]. Eckert, E. R. G., and Drake, R. M., 1972, Analysis of Heat and Mass Transfer, McGraw-Hill, New York.

[14]. R. Srinivasa Raju, Effects Of Soret And Dufour On Natural Convective Fluid Flow Past A Vertical Plate Embedded In Porous Medium In Presence Of Thermal Radiation Via FEM, Journal of the Korean Society for Industrial and Applied Mathematics, Vol. 20, No. 4, pp. 309 - 332, 2016.

[15]. J. Anand Rao, P. Ramesh Babu, R. Srinivasa Raju, Finite element analysis of unsteady MHD free convection flow past an infinite vertical plate with Soret, Dufour, Thermal radiation and Heat source, ARPN Journal of Engineering and Applied Sciences, Vol. 10, No. 12, pp. 5338 - 5351, 2015.

[16]. N. Ahmed, Soret and Radiation Effects on Transient MHD Free Convection From an Impulsively Started Infinite Vertical Plate, Journal of Heat Transfer, Vol. 134, pp. 062701-1 - 062701-9, 2012.

[17]. A. Postelnicu, Influence of magnetic field on heat and mass transfer from vertical surfaces in porous media considering Soret and Dufour effects, Int J Heat Mass Transf, 47 (2004), pp. 1467–1472.

[18]. D. Pal, H. Mondal, MHD non-Darcy mixed convective diffusion of species over a stretching sheet embedded in a porous medium with non-uniform heat source/sink, variable viscosity and Soret effect, Commun Nonlinear Sci Numer Simulat, 17 (2012), pp. 672–684.

[19]. M. K. Partha, Thermophoresis particle deposition in a non-Darcy porous medium under the influence of Soret, Dufour effects, Heat Mass Transf, 44 (2008), pp. 969–977.

[20]. T. Hayat, T. Muhammad, S.A. Shehzad, A. Alsaedi, Soret and Dufour effects in three-dimensional flow over an exponentially stretching surface with porous medium, chemical reaction and heat source/sink, Int J Numer Methods Heat Fluid Flow, 25 (4) (2015), pp. 762–7.

[21]. O.D. Makinde, P.O. Olanrewaju, Unsteady mixed convection with Soret and Dufour effects past a porous plate moving through a binary mixture of chemically reacting fluid, Chem Eng Commun, 198 (7) (2011), pp. 920–938.
[22]. O.D. Makinde, On MHD mixed convection with Soret and Dufour effects past a vertical plate embedded in a porous medium, Latin Am Appl Res, 41 (2011), pp. 63–68.
[23]. P.O. Olanrewaju, O.D. Makinde, Effects of thermal diffusion and diffusion thermo on chemically reacting MHD boundary layer flow of heat and mass transfer past a moving vertical plate with suction/injection, Arab J Sci Eng, 36 (2011), pp. 1607–1619.
[24]. O.D. Makinde, K. Zimba, O. Anwar Beg, Numerical study of chemically-reacting hydromagnetic boundary layer flow with Soret/Dufour effects and a convective surface boundary condition, Int J Thermal Environ Eng, 4 (1) (2012), pp. 89–98.
[25]. D. Pal, H. Mondal, Influence of chemical reaction and thermal radiation on mixed convection heat and mass transfer over a stretching sheet in Darcian porous medium with Soret and Dufour effects, Energy Convers Manage, 16 (2012), pp. 102–108 http://dx.doi.org/10.1016/j.enconman.2012.03.017.
[26]. M. Bourich, M. Hasnaoui, A. Amahmind, Soret convection in a shallow porous cavity submitted to uniform fluxes of heat and mass, Int Commun Heat Mass Transf, 31 (2004), pp. 773–782.
[27]. Dash, R. K., Mehta, K. N., Jayaraman, G.: Casson Fluid Flow in a Pipe Filled with a Homogeneous Porous Medium. Int. J. Eng. Sci. 34, 1145–1156 (1996).
[28]. Cogley, A. C., Vincentine, W. C., and Gilles, S. E., 1968, Differential Approximation for Radiative Transfer in a Non-Gray Gas Near Equilibrium," AIAA J., Vol. 6, pp. 551–555.